CHEMISTRY OF MATERIALS
Article

Chem. Mater. **2010,** *22,* 2491–2501 2491
DOI:10.1021/cm903127w

Self-Organized Thin Films of Hydrogen-Bonded Phthalocyanines: Characterization of Structure and Electrical Properties on Nanometer Length Scales

Niranjani Kumaran,[†] P. Alex Veneman, Britt A. Minch,[‡] Anoma Mudalige, Jeanne E. Pemberton, David F. O'Brien,[§] and Neal R. Armstrong*

Department of Chemistry, University of Arizona, Tucson, Arizona 85721. [†]Current Address: Intel Corp. 2501 NW 229th Ave, Hillsboro, Oregon 97124. [‡]Current Address: PPG Industries, PPG Coatings Innovation Center, 4335 Rosanna Dr., Allison Park, PA 15101. [§]Deceased.

Received October 9, 2009. Revised Manuscript Received February 1, 2010

We present the structural and electrical property characterization of solution-deposited thin films of a self-organizing phthalocyanine 2,3,9,10,16,17,23,24-octa(2-(4-octylbenzamide ethyl-sulfanyl) copper(II) phthalocyanine, Pc (**1**). Self-organization into columnar aggregates occurs mainly as a result of hydrogen bonding interactions between the benzamide groups in the side chains. These H-bonding interactions lead to ordered films of Pc (**1**), with the plane of the Pc parallel to the substrate plane, on gold surfaces modified with amide or amine functionalities, and on freshly cleaved highly order pyrolitic graphite (HOPG). Atomic force microscopy (AFM) confirms layer-by-layer growth for these Pc films up to coverages of ~10 monolayers, when deposition occurs from dilute solutions of the Pc. Conductive-tip AFM (C-AFM) measurements of these ordered Pc films, on modified Au and HOPG substrates, confirm the layered nature of these Pc films and show that the conductance decreases incrementally with the number of Pc monolayers being probed. On HOPG substrates, these measurements lead to an estimation of the conductance per Pc monolayer, and the Pc molecule−HOPG contact resistance of 8 MΩ, a value which is comparable with previously explored organic semiconductor materials.

Introduction

Cofacial columnar aggregates of discotic molecules, such as the hexabenzocoronenes (HBC), phthalocyanines (Pc), hexaazatriphenylene, porphyrines, and related materials can show high charge mobilities along the column axis, provided that these aggregates demonstrate good coherence lengths.[1−17] Hydrogen bonding groups incorporated into the cores of these molecules can aid in directing this aggregation and in some cases can assist in "templating" the deposition of ordered aggregates on various substrates.[12,13,18−24]

(1) Pisula, W.; Zorn, M.; Chang, J. Y.; Mullen, K.; Zentel, R. *Macromol. Rapid Commun.* **2009**, *30*, 1179–1202.
(2) Piot, L.; Marie, C.; Dou, X.; Feng, X.; Mullen, K.; Fichou, D. J. Am. Chem. Soc. **2009**, *131*, 1378-+.
(3) Feng, X. L.; Marcon, V.; Pisula, W.; Hansen, M. R.; Kirkpatrick, J.; Grozema, F.; Andrienko, D.; Kremer, K.; Mullen, K. *Nat. Mater.* **2009**, *8*, 421–426.
(4) Laschat, S.; Baro, A.; Steinke, N.; Giesselmann, F.; Hagele, C.; Scalia, G.; Judele, R.; Kapatsina, E.; Sauer, S.; Schreivogel, A.; Tosoni, M. *Angew. Chem., Int. Ed.* **2007**, *46*, 4832–4887.
(5) Simpson, C. D.; Wu, J. S.; Watson, M. D.; Mullen, K. *J. Mater. Chem.* **2004**, *14*, 494–504.
(6) de Heer, W. A.; Berger, C.; Wu, X. S.; First, P. N.; Conrad, E. H.; Li, X. B.; Li, T. B.; Sprinkle, M.; Hass, J.; Sadowski, M. L.; Potemski, M.; Martinez, G. *Solid State Commun.* **2007**, *143*, 92–100.
(7) De Cupere, V.; Tant, J.; Viville, P.; Lazzaroni, R.; Osikowicz, W.; Salaneck, W. R.; Geerts, Y. H. *Langmuir* **2006**, *22*, 7798–7806.
(8) Wohrle, D.; Kreienhoop, L.; Schnurpfeil, G.; Elbe, J.; Tennigkeit, B.; Hiller, S.; Schlettwein, D. *J. Mater. Chem.* **1995**, *5*, 1819–1829.
(9) Smolenyak, P.; Peterson, R.; Nebesny, K.; Torker, M.; O'Brien, D. F.; Armstrong, N. R. *J. Am. Chem. Soc.* **1999**, *121*, 8628–8636.
(10) Zangmeister, R. A. P.; Smolenyak, P. E.; Drager, A. S.; O'Brien, D. F.; Armstrong, N. R. *Langmuir* **2001**, *17*, 7071–7078.
(11) Minch, B. A.; Xia, W.; Donley, C. L.; Hernandez, R. M.; Carter, C.; Carducci, M. D.; Dawson, Al; O'Brien, D. F.; Armstrong, N. R. *Chem. Mater.* **2005**, *17*, 1618–1627.
(12) Gearba, R. I.; Lehmann, M.; Levin, J.; Ivanov, D. A.; Koch, M. H. J.; Barbera, J.; Debije, M. G.; Piris, J.; Geerts, Y. H. *Adv. Mater.* **2003**, *15*, 1614–1618.
(13) Shirakawa, M.; Kawano, S.; Fujita, N.; Sada, K.; Shinkai, S. *J. Org. Chem.* **2003**, *68*, 5037–5044.
(14) Sergeyev, S.; Pisula, W.; Geerts, Y. H. *Chem. Soc. Rev.* **2007**, *36*, 1902–1929.
(15) Tylleman, B.; Gbabode, G.; Amato, C.; Buess-Herman, C.; Lemaur, V.; Cornil, J.; Aspe, R. G.; Geerts, Y. H.; Sergeyev, S. *Chem. Mater.* **2009**, *21*, 2789–2797.
(16) Sergeyev, S.; Levin, J.; Balandier, J. Y.; Pouzet, E.; Geerts, Y. H. *Mendeleev Commun.* **2009**, *19*, 185–186.
(17) Pouzet, E.; De Cupere, V.; Heintz, C.; Andreasen, J. W.; Breiby, D. W.; Nielsen, M. M.; Viville, P.; Lazzaroni, R.; Gbabode, G.; Geerts, Y. H. *J. Phys. Chem. C* **2009**, *113*, 14398–14406.
(18) Wasserfallen, D.; Fischbach, I.; Chebotareva, N.; Kastler, M.; Pisula, W.; Jackel, F.; Watson, M. D.; Schnell, I.; Rabe, J. R.; Spiess, H. W.; Mullen, K. *Adv. Funct. Mater.* **2005**, *15*, 1585–1594.
(19) Kim, J. Y.; Lee, K.; Coates, N. E.; Moses, D.; Nguyen, T. Q.; Dante, M.; Heeger, A. J. *Science* **2007**, *317*, 222–225.
(20) Paraschiv, I.; Tomkinson, A.; Giesbers, M.; Sudholter, E. J. R.; Zuilhof, H.; Marcelis, A. T. M. *Liq. Cryst.* **2007**, *34*, 1029–1038.
(21) Foster, E. J.; Lavigueur, C.; Ke, Y. C.; Williams, V. E. *J. Mater. Chem.* **2005**, *15*, 4062–4068.
(22) Ma, H.; Luo, J.; Kang, S. H.; Wong, S.; Kang, J. W.; Jen, A. K.-Y.; Barto, R.; Frank, C. W. *Macromol. Rapid Commun.* **2004**, *25*, 1667–1673.
(23) Palma, M.; Levin, J.; Debever, O.; Geerts, Y.; Lehmann, M.; Samori, P. *Soft Matter* **2008**, *4*, 303–310.
(24) Piot, L.; Marchenko, A.; Wu, J. S.; Mullen, K.; Fichou, D. *J. Am. Chem. Soc.* **2005**, *127*, 16245–16250.

Published on Web 03/16/2010

Achieving alignment of columar aggregates with coherence lengths in excess of several hundred nanometers has been achieved by Langmuir−Blodgett deposition,[9] zone casting,[25] zone crystallization,[26] drop casting onto polytetrafluoroethylene rubbed surfaces,[12] and recently, templating from self-assembled monolayers.[2] Achieving aggregates with the plane of the discotic molecule parallel to the substrate plane (face-on alignment, the preferred orientation for organic solar cell applications of these materials),[5,27−29] is significantly more challenging.[7,14−16,30−32] Several attempts have been made to align disk-like molecules parallel to the substrate plane by tailoring molecular structure or the functional groups in the side chains. It has been postulated that the presence of heteroatoms near the disk periphery of discotic molecules is the key for face-on alignment.[30,31,33,34] Pisula et al. have made extensive structural studies with modifications of HBC, having different core sizes and side chain lengths and complexities.[1,3,30] Bulky branched side chains facilitated face-on alignment from melts by drastically decreasing the isotropization temperature, however, such side chains tended to introduce intracolumnar disorder in higher coverage films because of steric crowding.[1,3,30]

In addition to these structural investigations, several attempts have been made to find proper deposition techniques that would yield molecules lying parallel to the substrate plane. Deposition of liquid crystalline materials from their molten state between two glass plates was demonstrated; however, the desired face-on alignment was not retained after separation of one plate.[7,30,31,35,36] Rabe and co-workers reported solution processed homeotropic alignment of HBC molecules on HOPG and MoS_2 in which formation of thicker films required controlling the temperature of the substrate and solution to prevent precipitation.[37−39] Vacuum vapor deposition and molecular beam epitaxy of crystalline dyes has been employed by various research groups to achieve ordered multilayers with the plane of the molecule parallel to the substrate, however, even for Pc moleculess with layered bulk structures, ordering is typically extended to only a few molecular layers.[40−45] Geerts and co-workers have recently adopted the use of a "sacrificial polymer layer", which provides guidance for homeotropic alignment of liquid crystalline Pc assemblies, much as was shown previously through the use of parallel glass plates, but with a removable top layer.[17,46] Interestingly annealing of these structures, after the sacrificial layer was removed, suggested reintroduction of disorder into these films, since intermolecular forces are quite weak in these LC−Pc systems, and homeotropically aligned layers may exhibit "lattice strain" if their structures deviate significantly from stable bulk crystal structures.[40]

Here we show that deposition from extremely dilute solutions allow for the formation of ordered, layered, phthalocyanine films, for 2,3,9,10,16,17,23,24-octa(2-(4-octylbenzamide ethyl-sulfanyl) phthalocyanato copper-(II), Pc (**1**) (Figure 1). This Pc has been modified with hydrogen bonding benzamide groups in the side chains, placed internally in the side chains, to promote intracolumn, but not intercolumn, interactions. Our studies show that if interactions with the substrate material (chemically modified Au or freshly cleaved HOPG) are strong, and if deposition rates are low enough to allow for molecule−substrate interactions to dominate over molecule−molecule interactions, flat-lying monolayers of these discotic materials can be achieved. For deposition of the second and subsequent monolayers of material, deposition rates need to be low enough, and molecule−molecule interactions large enough, to allow for the initially deposited monolayer to "template" the deposition of the second layer.

Ultrasmooth gold (template-stripped gold, TSG) substrates, modified with self-assembled monolayers containing amide terminal functional groups provided for formation of layered Pc films, consistent with layer-by-layer film growth dominated by H-bonding. Polarization modulated FT-IR (PM-IRRAS) studies confirm this orientation and the nature of the H-bonding interactions between the first deposited Pc layers and the chemically modified substrate. Well ordered, layered thin films were also achieved by solution deposition on HOPG. Less ordered layered Pc films were also obtained on ITO

(25) Tracz, A.; Jeszka, J. K.; Watson, M. D.; Pisula, W.; Mullen, K.; Pakula, T. *J. Am. Chem. Soc.* **2003**, *125*, 1682–1683.
(26) Ioannidis, A.; Dodelet, J. P. *J. Phys. Chem. B* **1997**, *101*, 891–900.
(27) Schmidtke, J. P.; Friend, R. H.; Kastler, M.; Mullen, K. *J. Chem. Phys.* **2006**, 124.
(28) Huijser, A.; Suijkerbuijk, B. M. J. M.; Gebbink, R. J. M. K.; Savenije, T. J.; Siebbeles, L. D. A. *J. Am. Chem. Soc.* **2008**, *130*, 2485–2492.
(29) Sullivan, P.; Jones, T. S.; Ferguson, A. J.; Heutz, S. *Appl. Phys. Lett.* **2007**, 91.
(30) Pisula, W.; Tomovic, Z.; El Hamaoui, B.; Watson, M. D.; Pakula, T.; Mullen, K. *Adv. Funct. Mater.* **2005**, *15*, 893–904.
(31) Hatsusaka, K.; Ohta, K.; Yamamoto, I.; Shirai, H. *J. Mater. Chem.* **2001**, *11*, 423–433.
(32) Gearba, R. I.; Anokhin, D. V.; Bondar, A. I.; Bras, W.; Jahr, M.; Lehmann, M.; Ivanov, D. A. Adv. Mater. **2007**, *19*, 815−820.
(33) Terasawa, N.; Monobe, H.; Kiyohara, K.; Shimizu, Y. *Chem. Commun.* **2003**, 1678–1679.
(34) Randriamahazaka, H.; Plesse, C.; Teyssie, D.; Chevrot, C. *Electrochem. Commun.* **2003**, *5*, 613–617.
(35) Cohen, R.; Kronik, L.; Shanzer, A.; Cahen, D.; Liu, A.; Rosenwaks, Y.; Lorenz, J. K.; Ellis, A. B. *J. Am. Chem. Soc.* **1999**, *121*, 10545–10553.
(36) Fujikake, H.; Murashige, T.; Sugibayashi, M.; Ohta, K. *Appl. Phys. Lett.* **2004**, *85*, 3474–3476.
(37) Friedlein, R.; Crispin, X.; Simpson, C. D.; Watson, M. D.; Jackel, F.; Osikowicz, W.; Marciniak, S.; de Jong, M. P.; Samori, P.; Jonsson, S. K. M.; Fahlman, M.; Mullen, K.; Rabe, J. P.; Salaneck, W. R. *Phys. Rev. B* **2003**, *68*, 195414.
(38) Samori, P.; Keil, M.; Friedlein, R.; Birgerson, J.; Watson, M.; Mullen, M.; Salaneck, W. R.; Rabe, J. P. *J. Phys. Chem. B* **2001**, *105*, 11114–11119.
(39) Mullen, K.; Rabe, J. P. *Acc. Chem. Res.* **2008**, *41*, 511–520.
(40) Hooks, D. E.; Fritz, T.; Ward, M. D. Adv. Mater. **2001**, *13*, 227-+.
(41) Walzer, K.; Toccoli, T.; Pallaoro, A.; Iannotta, S.; Wagner, C.; Fritz, T.; Leo, K. *Surf. Sci.* **2006**, *600*, 2064–2069.
(42) England, C. D.; Collins, G. E.; Schuerlein, T. J.; Armstrong, N. R. *Langmuir* **1994**, *10*, 2748–2756.
(43) Anderson, M. L.; Williams, V. S.; Schuerlein, T. J.; Collins, G. E.; England, C. D.; Chau, L. K.; Lee, P. A.; Nebesny, K. W.; Armstrong, N. R. *Surf. Sci.* **1994**, *309*, 551–558.
(44) Walzer, K.; Toccoli, T.; Pallaoro, A.; Pallaoro, A.; Verucchi, R.; Fritz, T.; Leo, K.; Boschetti, A.; Iannotta, S. *Surf. Sci.* **2004**, *573*, 346–358.
(45) Schafer, A. H.; Seidel, C.; Fuchs, H. Adv. Funct. Mater. **2001**, *11*, 193−197.
(46) Gregg, B. A.; Fox, M. A.; Bard, A. J. *J. Phys. Chem.* **1990**, *94*, 1586–1598.

surfaces, and on ITO modified with thin films of PEDOT:PSS, a common conductive polymer dispersion used as the base layer in many different organic solar cell and organic light emitting diode technologies.

Conductive-tip AFM studies of these ordered films, up to coverages of ~10 monolayers of the Pc, were conducted using Pt/Ir tips (to ensure ohmic contacts between the tip and the Pc layers). On HOPG, we were able to characterize the current−voltage behavior of these ultrathin Pc layers, where the current density at any bias varied systematically with the overall thickness of the Pc layer, up to a maximum of 10 Pc layers. In the ohmic region, the contact resistance, per Pc molecule was estimated, and was found to be in the range reported previously for layered crystalline organic semiconductors. These studies provide the impetus for the formation of organic solar cells based on layers of Pc (**1**) as the primary photoactive, donor layer.

Experimental Section

Materials. The following chemicals and substrates were used as provided: 11-mercaptoundecanoic acid (Aldrich), 3-aminopropyltriethoxysilane (APTES) (Aldrich), *N*-hydroxysuccinimide(NHS) (Aldrich), 1-ethyl-3(3-dimethylaminopropyl)carbodiimide hydrochloride (EDC) (Fluka), *n*-propylamine (Alfa Aesar), HEPES buffer (Electron Microscopy Sciences), EPO-TEK 353ND-4 part A and part B (Epoxy Technology), PEDOT:PSS (Baytron), HPLC grade $CHCl_3$ (EMD Chemicals Inc.), ethanol (Decon Laboratories, Inc.), gold shots (Kurt J. Lesker), mica (Ted Pella Inc.), glass slides (VWR Micro slides), and ITO (Colorado Concept Coatings Limited, sheet resistance ca. 13 Ω/cm^2).

Scheme S1 in the Supporting Information shows the synthetic route to 2,3,9,10,16,17,23,24-octa(2-(4-octylbenzamide ethylsulfanyl) CuPc (**1**), a modification of the previously reported synthesis of 2,3,9,10,16,17,23,34-octakis(2-benzyloxyethyl-sulfanyl) copper(II) phthalocyanine.[11] NMR (1D ^1H and 2D [$^1H-^{13}C$]-HSQC), MALDI-MS, FT-IR, elemental analysis, and solution absorbance data are detailed in the Supporting Information.

Surface Modification and Thin Film Deposition. *Preparation of Template Stripped Gold (TSG) Substrates.* Gold substrates were prepared using the method described by Wagner et al.[47] Two hundred nanometer gold films were vapor-deposited at a rate of 1 Å/s onto freshly cleaved mica sheets that had been pre-annealed at 300 °C for 12 h at a pressure of 10^{-6} Torr. The gold film was then annealed for 6 h at the same pressure and temperature. The gold/mica sheets were then glued to clean glass slides (EPO-TEK 353ND-4 part A/part B = 5:1) and cured at 150° for one hour. The mica was then mechanically stripped using scotch tape to provide a clean gold surface, which tapping mode AFM characterization showed an rms roughness of ca. 1 Å.

Formation of Self-Assembled Monolayers on Gold and the Subsequent Amide-Coupling Reaction. TSG slides were immersed in 1 mM ethanolic solution of 11-mercaptoundecanoic acid (MUA) for 12 h, rinsed in ethanol, and dried in a stream of nitrogen. These carboxylic acid terminated surfaces were converted to a simple amide as described elsewhere.[48,49] The amide bond-forming reaction was mediated by NHS/EDC to transform the terminal carboxylic acid groups into activated NHS esters. The MUA-modified Au surface was activated using an aqueous mixture of 15 mM N-hydroxysuccinimide (NHS) and 75 mM 1-ethyl-3 (3-dimethylaminopropyl) carbodiimide hydrochloride (EDC) for 30 min. The resultant MUS-NHS ester monolayer was reacted for 30 min with 10 mM n-propylamine in HEPES buffer (0.1M, pH 7.0). After the reaction, the slides were rinsed in water and dried with a stream of nitrogen.

Preparation of Pc Films on Amide Functionalized Gold (Au/SAM/Pc). Amide-functionalized TSG substrates were soaked in 10^{-6}M solutions of Pc (**1**) in $CHCl_3$ for various times. Following adsorption, substrates were rinsed in $CHCl_3$ and blow dried with nitrogen.

Preparation of Pc Films on HOPG (HOPG/Pc): Freshly cleaved HOPG was soaked in 10^{-6} M Pc in $CHCl_3$ for up to one hour and then rinsed with $CHCl_3$ and blown dry with nitrogen before imaging.

Preparation of Pc Films on ITO (ITO/Pc). ITO was cleaned as discussed above with detergent/solvent cleaning, followed by treatment with an O_2 plasma (Harrick) at 60W for 15 min, followed by immersion in 10^{-6} M Pc (**1**) in $CHCl_3$ for up to hour and rinsing with $CHCl_3$.

Preparation of Pc Films on PEDOT:PSS Modified ITO (ITO/PEDOT:PSS/Pc):. Indium−tin oxide (ITO) (Colorado Concepts, Sn/In = ~1:10; ~15/sq) was cleaned by previously described detergent/solvent ultrasonic procedures.[50] Each ITO piece was subsequently briefly etched by flooding with 6 M HCl/0.2 M $FeCl_3$ for 10 s, followed by spinning at a rate of 3000 rpm while rinsing with copious amount of water. Acid-activated ITO was immediately flooded with the PEDOT:PSS solution (Baytron P) for 6 s, followed by spinning at a rate of 3000 rpm for 1 min. It was then blown dry with a stream of nitrogen. The PEDOT:PSS modified ITO slide was next soaked in 10^{-6}M Pc (**1**) solution in $CHCl_3$ for up to one hour, followed by rinsing with $CHCl_3$ and drying with a stream of nitrogen.

Characterization Techniques. *UV−vis Spectroscopy.* UV−vis spectrophotometer (S1400 series, Spectral Instruments) with a CCD array was used for the absorbance studies. Absorbance of Pc (**1**) in chloroform, in 1.0 cm path length quartz cuvettes were measured at various concentrations. A deuterium (D_2) lamp and a tungsten

(47) Wagner, P.; Hegner, M.; Guntherodt, H. J.; Semenza, G. *Langmuir* **1995**, *11*, 3867–3875.

(48) Leon, J. W.; Kawa, M.; Fréchet, J. M. J. *J. Am. Chem. Soc.* **1996**, *118*, 8847–8859.

(49) Yang, C.; Mertz, J. *Opt. Lett.* **2003**, *28*, 224–226.

(50) Marrikar, F. S.; Brumbach, M.; Evans, D. H.; Lebron-Paler, A.; Pemberton, J. E.; Wysocki, R. J.; Armstrong, N. R. *Langmuir* **2007**, *23*, 1530–1542.

lamp were employed as UV and visible wavelength sources, respectively.

X-ray Diffraction (*XRD*). XRD measurements of power samples were performed with a PANalytical X'Pert PRO MPD system equipped with a copper (Kα) radiation (λ = 1.54 Å) source, a spinner sample stage, and a real time multiple strip X-ray detector, x'celerator. The instrument was operated at 50 KV and 40 mA target current to record the $\theta-2\theta$ continuous scan with a step size of 0.0167°. A fixed divergent slit of 1/16° was used in the incident beam optics, followed by an antiscattering slit of 1/8°. Pattern indexing and unit cell refinement were done with X'Pert Plus (version 1.0) supplied by Philips Analytical.

For the temperature dependent X-ray measurements, a temperature controlled chamber was PreFix mounted onto a vertical X'Pert PRO goniometer. Powder of Pc (**1**) was kept on a homogenously heated sample stage. Temperature was controlled with Anton Paar temperature controller (TCU 50). The system was programmed to heat and cool. The sample was equilibrated for 5 min at desired temperatures before acquisition of data.

Atomic Force Microscopy (*AFM*) *and Conducting Probe AFM* (*C-AFM*). AFM images and current−voltage behavior (I/V) were both obtained with a Dimension 3100 Nanoscope IV system (Veeco Metrology Group, Santa Barbara, CA). Tapping mode images were recorded in air with oxide-sharpened silicon nitride tips with a nominal spring constant of 40 N/m and a resonance frequency of 325 kHz. All the images were recorded with a resolution of 512 × 512 data points.

For C-AFM characterization, images and $I-V$ curves were recorded in air with an ultra sharp conducting Pt−Ti tip (CSC38, MikroMasch) having a spring constant in the range of 0.03−0.08 N/m and a resonance frequency of 10−20 kHz. The sample was electrically connected to ground with silver paint around the edges of each substrate. Height and current images were first collected in the normal AFM imaging mode using the conducting probe. The area of interest was selected by zooming the height image and then scan size was dropped to 0 nm to acquire the $I-V$ traces by a point contact method. Setting the scan size at 0 nm, keeps the tip at the center of the imaging area, which is the (0,0) coordinate. At this point the Nanoscope software was switched to force calibration mode and the sample bias was set to 0 V. After acquiring an $I-V$ plot at the (0,0) coordinate, the x and y coordinate were changed appropriately to move the tip to a new position. In this way a multitude of I/V plots could be obtained over a statistically meaningful number of regions of the Pc film. For the determination of contact resistance, the tip was programmed to acquire $I-V$ plots at several points separated by ∼5 nm, periodically sampled across the HOPG/Pcsample. Full details of this imaging/electrical property characterization technique are presented elsewhere in the context of discussions of the electrical properties of ITO electrodes and those same electrodes coated with thin Pc films.[51]

Fourier Transform Infrared Spectroscopy (*FTIR*). Transmission FTIR spectra were obtained on a Magna-IR, Series II System 550 FTIR instrument (Nicolet Instrument Corporation) equipped with a globar IR source (EverGlo) and liquid nitrogen cooled MCT detector. Each spectrum is an average of 512 scans at a resolution of 2 cm^{-1}. Data collection and analysis were done by Omnic 7.3 provided by Thermo Electron Corporation. For this analysis, a thin transparent KBr pellet was made by grinding a small amount of Pc (**1**) (∼1% by weight vs KBr).

For the variable-temperature IR measurements, the powder sample was heated to the desired temperatures in a vacuum annealing chamber, while controlling temperatures with CN4800 series temperature controller (Omega Technologies Company) and then KBr pellets were made from the heated powders for the analysis.

Polarization-Modulation Fourier Transform Infrared Reflection−Absorption Spectroscopy (*PM-FT-IRRAS*). Thin films of Pc (**1**) on amide-functionalized TSG substrates were used to acquire PM-FT-IRRAS spectra. Spectra were acquired with Nicolet Nexus 670-FTIR Spectrometer with dual channel capability, equipped with an external optical bench (TOM, table-top optical module), liquid nitrogen cooled MCT detector (Thermo Electron Scientific Corporation), Photoelastic Modulator (PEM) (Hinds Instruments PM-90 with ZnSe 50 kHz optical head), and demodulator (GWC Instruments Synchronous Sampling Demodulator). Spectra of 2000 scans at 4 cm^{-1} resolution were recorded in a range of 4000−700 cm^{-1}. The PM-FT-IRRAS differential reflectance ($\%\Delta R/R$) values were converted to absorbance units for comparison with conventional FTIR data.

Results and Discussion

Synthesis of Pc (1). The synthesis and basic characterization of Pc (**1**) (Figure 1) is detailed in the Supporting Information (Scheme I). Pc (**1**) is a variation on a previous octa-thioether phthalocyanine, 2,3,9,10,16,17,23,34-octakis(2-benzyloxyethyl-sulfanyl) copper(II) phthalocyanine,[11] incorporating eight alkyl terminated benzamide-thio-ether side chains. Amide groups known to promote cofacial self-assembly were placed in the interior of the side chain to minimize cross-column interactions. Octyl chains were introduced in the 4-position of the terminal phenyl groups to enhance the solubility of Pc (**1**) in solvents, such as THF and chloroform.

Mild synthetic conditions afford the phthalonitrile. 4-Octyl benzoyl chloride was coupled to 2-chloroethylamine hydrochloride, the chloride was displaced with potassium thioacetate, modifying a procedure which removes the acetyl protecting group under basic conditions, in high yields. The resultant thiol was coupled

(51) Veneman, P. A. Ph.D. Dissertation, University of Arizona, **2009**.

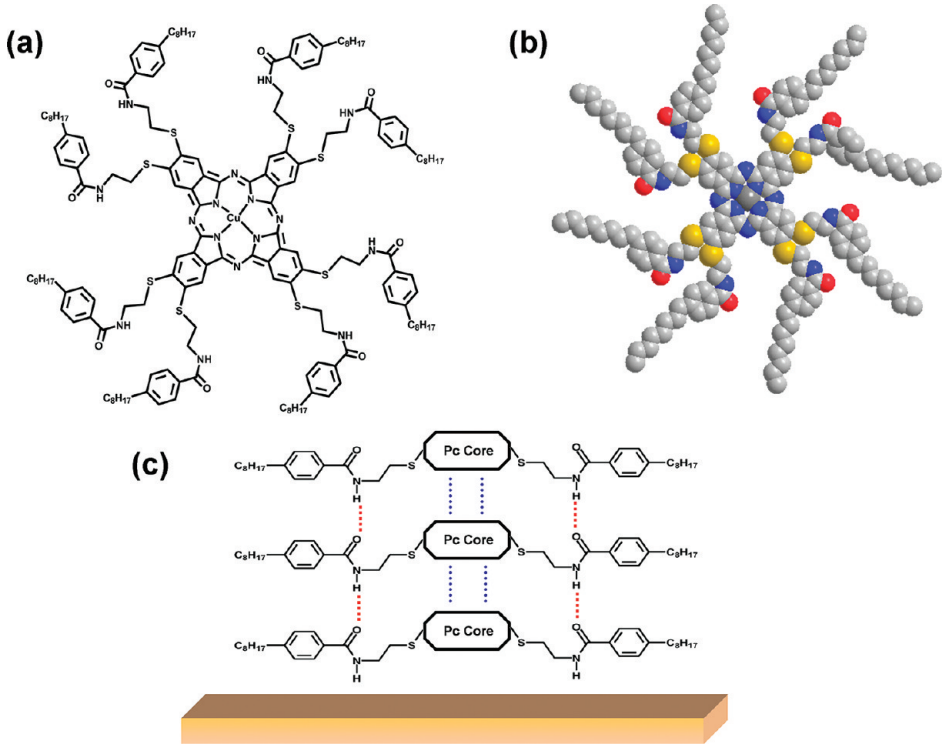

Figure 1. (a) Chemical structure of 2,3,9,10,16,17,23,24-octa(2-(4-octylbenzamide ethylsulfanyl) phthalocyanato copper(II), Pc (**1**). (b) Space filling model of the molecule in its minimal energy configuration. (c) Schematic view of the aggregation of the molecules through hydrogen bondings exerted via amide units in the side chains, $\pi-\pi$ stacking between the aromatic rings and S−S interactions.

to 4,5-diclorophthalonitrile at room temperature in DMSO (c). The phthalocyanine was then prepared via established condensation protocols.[52−55]

Structural Characterization of Pc (1). The Q-band absorbance for monomeric Pc (**1**) (λ_{max} = 712 nm in chloroform, $\varepsilon = 1.1 \times 10^5\ M^{-1}\ cm^{-1}$) is dominant only at concentrations below $\sim 10^{-6}$ M. The blue-shifted shoulder in solution Q-band spectra and in thin film formats (Figure 2a) is consistent with strong cofacial aggregation of these Pc moieties.[56,57] Addition of 3% v/v trifluoromethane sulfonic acid to $\sim 5 \times 10^{-6}$ M solutions of Pc (**1**) disrupts this aggregation, reforming a monomer absorbance band at ~800 nm, as expected if H-bonding is the principal mode of interaction (Figure S2, Supporting Information).

Differential scanning calorimetry of powders of Pc harvested from chloroform show an endothermic isotropization transition at 243.1 °C with an enthalpy of isotropization of 82 KJ/mol during the first scan (Figure 2b). The high isotropization temperature and enthalpy of isotropization are believed to be associated with strong intermolecular H-bonding interactions.[58] After the first DSC scan, a weak, reversible phase transition was observed between 174.2 and 182.6 °C. Decomposition of the Pc was noted above temperatures of ~300 °C.

Figure 3 shows X-ray diffraction data for powders of Pc (**1**) harvested from chloroform. These diffraction features were indexed to an orthorhombic unit cell (a = 42.3 Å, b = 18.1 Å, c = 4.5 Å, volume = 3490.5 Å^3) including diffractions from the (100), (010), and (010) planes. The sharp, high intensity Bragg peak arising at $d = 41.8 \pm 0.3$ Å is consistent with parallel Pc columns and a Pc edge-to-edge (column−column) distance of ~42 Å, which is smaller than expected from fully extended side chains and presumably arises from side chain compression. The Pc−Pc cofacial stacking distance of 4.5 Å (along the c-axis), are dimensions expected from macrocycle−macrocycle interactions dictated by H-bonding between the Pc rings, in close agreement with the average H-bonding distances previously observed in other H-bonded molecular assemblies.[13,58−61] An additional monoclinic phase is also present at ~10% of the intensity of the orthorhombic phase, sharing the main Bragg peak (a = 42.9 Å, b = 3.6 Å, c = 18.3 Å; $\alpha = \gamma = 90°$, $\beta = 100.4°$; volume = 2814.5 Å^3),

(52) Tomoda, H.; Saito, S.; Shiraishi, S. *Chem. Lett*. **1983**, 313–316.
(53) Petritsch, K.; Friend, R. H.; Lux, A.; Rozenberg, G.; Moratti, S. C.; Holmes, A. B. *Synth. Met*. **1999**, *102*, 1776–1777.
(54) Lux, A.; Rozenberg, G. G.; Petritsch, K.; Moratti, S. C.; Holmes, A. B.; Friend, R. H. *Synth. Met*. **1999**, *102*, 1527–1528.
(55) Svedhem, S.; Hollander, C. A.; Shi, J.; Konradsson, P.; Liedberg, B.; Svensson, S. C. T. *J. Org. Chem*. **2001**, *66*, 4494–4503.
(56) Chau, L. K.; England, C. D.; Chen, S. Y.; Armstrong, N. R. *J. Phys. Chem*. **1993**, *97*, 2699–2706.
(57) Schmidt, A.; Schlaf, R.; Louder, D.; Chau, L. K.; Chen, S. Y.; Fritz, T.; Lawrence, M. F.; Parkinson, B. A.; Armstrong, N. R. *Chem. Mater*. **1995**, *7*, 2127–2135.
(58) Paraschiv, I.; Giesbers, M.; van Lagen, B.; Grozema, F. C.; Abellon, R. D.; Siebbeles, L. D. A.; Marcelis, A. T. M.; Zuilhof, H.; Sudholter, E. J. R. *Chem. Mater*. **2006**, *18*, 968–974.
(59) Hartgerink, J. D.; Granja, J. R.; Milligan, R. A.; Ghadiri, M. R. *J. Am. Chem. Soc*. **1996**, *118*, 43–50.
(60) Nguyen, T. L.; Fowler, F. W.; Lauher, J. W. *J. Am. Chem. Soc*. **2001**, *123*, 11057–11064.
(61) Schoonbeek, F. S.; van Esch, J. H.; Wegewijs, B.; Rep, D. B. A.; de Haas, M. P.; Klapwijk, T. M.; Kellogg, R. M.; Feringa, B. L. *Angew. Chem., Int. Ed*. **1999**, *38*, 1393–1397.

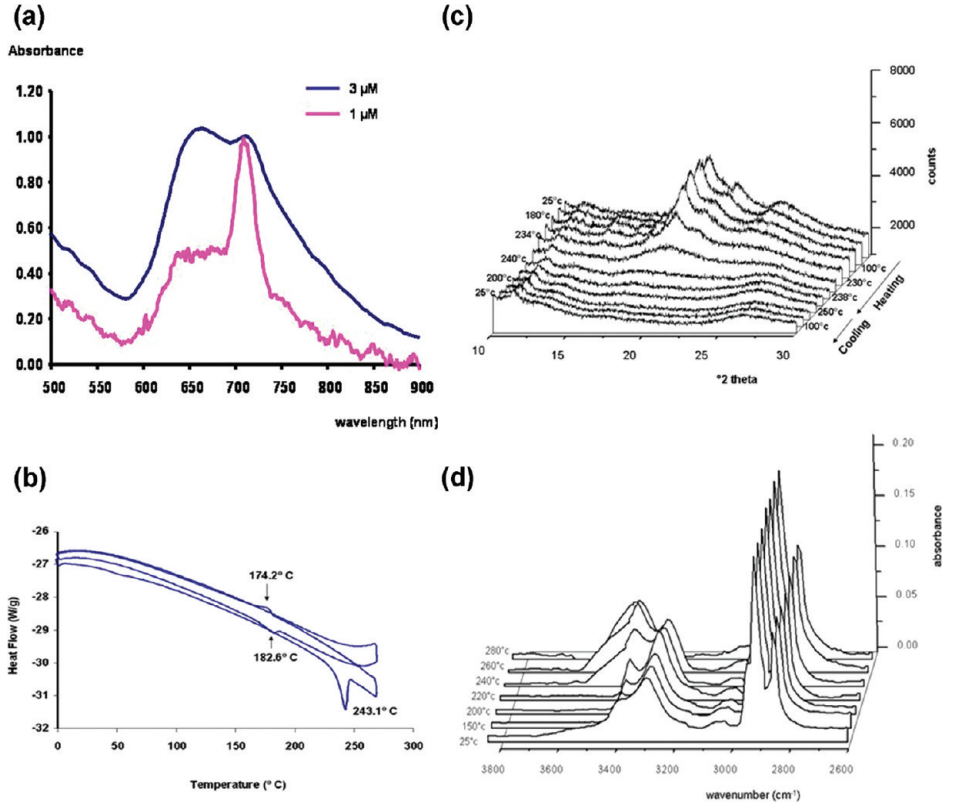

Figure 2. (a) Normalized visible absorbance spectrum of Pc (**1**) in $CHCl_3$ at 1×10^{-6} and 3×10^{-6} M showing onset of cofacial aggregation. (b) DSC scans of powders of Pc (**1**) during two heating−cooling cycles between 0 and 280 °C. (c) X-ray diffraction pattern of powders of Pc (**1**), at different temperatures during a heating−cooling cycle, showing disturbed intracolumnar order above the isotropization temperature. (d). FTIR spectrum of pelletized Pc (**1**) at variable temperatures, the N−H stretching peaks shifts toward high wavenumbers upon disruption of intermolecular hydrogen bonds above ~240 °C.

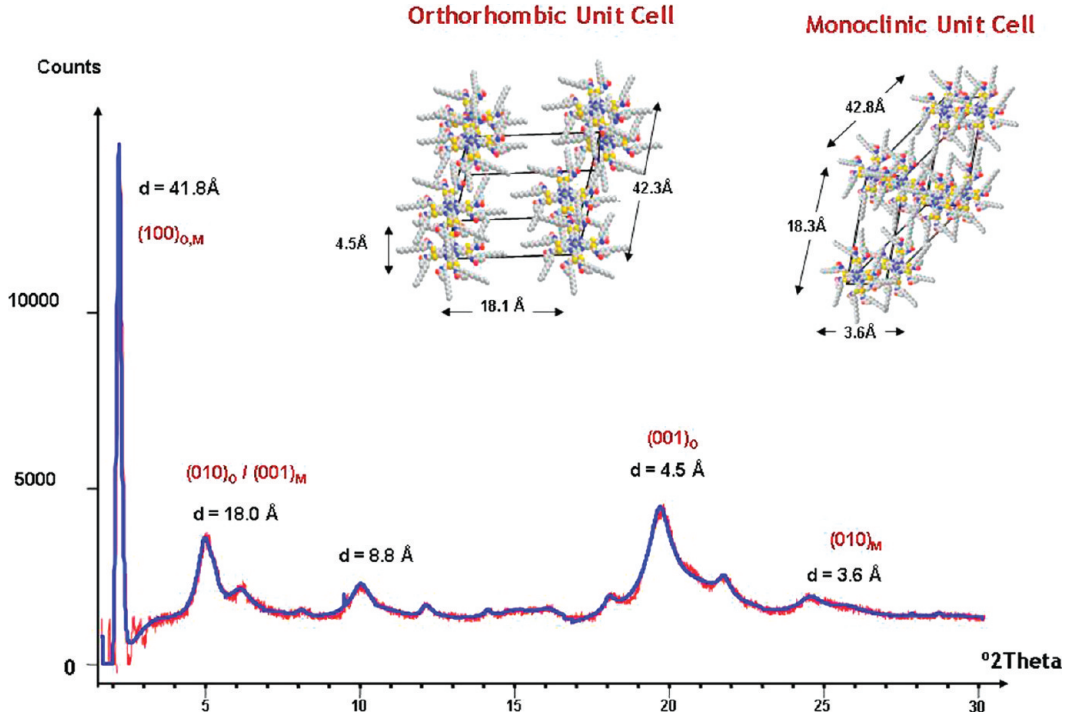

Figure 3. XRD for powders of Pc (**1**) harvested from chloroform. A dominant orthorhombic unit cell (90% of diffracted intensity) is easily indexed, and an additional small set of diffraction features can be indexed to a monoclinic cell (10% of diffracted intensity). In the dominant orthorhombic cell, a Pc−Pc stacking distance (cofacial) of 4.5 Å is observed; for the monoclinic cell the Pc−Pc stacking distance is 3.6 Å. Pc rings are shown schematically in the inset and are not to scale. Blue line = fit; red line = raw data; O = orthorhombic cell; M = monoclinic.

accommodating closer Pc−Pc contacts. Such a monoclinic unit cell would be expected from Pc aggregation mainly governed by $\pi-\pi$ and S−S interactions, instead of H-bonding interactions, allowing for closer Pc−Pc cofacial

interaction.[11,62,63] We hypothesize that this variability in interactions between adjacent Pcs is due to the presence of the cis−trans geomeries of adjacent amide bonds, as observed for other H-bonded assemblies.[64−66] Pc molecules with *trans*-amide isomer units in the side chains (the major isomer indicated by NMR, see Supporting Information) are expected to provide for intermolecular H-bonds, leading to the dominant orthorhombic geometry. The small fraction of Pc molecules possessing the *cis*-amide unit in eight side chain positions would be expected to pack through $\pi-\pi$ or S−S interactions in the monoclinic structure, where efficient H-bonding interaction is hindered.[64−66]

IR spectra of powders of Pc (**1**) harvested from chloroform and dispersed in KBr pellets (Figure S3, Supporting Information) show a broad N−H stretching band at $\sim$ 3295 cm^{-1}, and amide I and amide II bands at 1654 cm^{-1}, and 1537 cm^{-1} respectively, indicative of H-bonded network assemblies.[13,58,59,64] Heating these pelletized powders of (**1**) above ~250 °C disrupts these H-bonding interactions, as evidenced by shifts in the υ_{N-H} band to higher frequencies (Figure 2d). A small shoulder at 3398 cm^{-1} shows the existence of non-hydrogen-bonded N−H groups resulting from Pc units not involved in H-bonding (e.g., the *cis*-amide units).

Temperature-dependent XRD (Figure 2c) showed the loss of the $(001)_O$ (d = 4.5 Å) and the $(010)_M$ (d = 3.6 Å) reflections above 238 °C, consistent with the loss of intracolumnar order, and consistent with the temperature dependent FT-IR data.[12] Upon cooling, diffraction peaks associated with intracolumnar order were not recovered, that is, once weakened the H-bonding interactions apparently do not reform at lower temperatures, which is likely the result of side-chain reorganization.

Adsorption of Pc (1) on Au and HOPG. Thin films of Pc (**1**) were drop cast or adsorbed on a variety of substrates with various solution concentrations, solvents, and deposition conditions in order to understand the factors that lead to face-on alignment. Deposition from solutions above $\sim 10^{-6}$ M leads generally to crystalline deposits which AFM imaging showed to possess layer planes separated by ca. 18−20 Å, close to the *b*-axis dimension of the orthorhombic unit cell and the *c*-axis dimension of the monoclinic unit cell (Supporting Information, Figure S7b).[67]

We were able to achieve structured thin films of Pc (**1**), with the plane of the Pc parallel to the substrate plane, on template-stripped Au surfaces (TSG-Au) which had been chemically modified with an amide-terminated alkanethiol monolayer, bis(trimethoxysilylpropyl)urea.[67] For these depositions Pc (**1**) was chemisorbed from a $\sim 10^{-6}$ M solution, a concentration we found necessary to achieve well ordered, layered structures with reasonable coherence lengths. AFM images of separated islands achieved after 15 min of chemisorption (Figure 4) suggest Pc layer planes separated by multiples of 4−5 Å, (*c*-axis dimension of the orthorhombic unit cell), consistent with layer-by-layer film growth controlled by H-bonding, with the plane of the Pc parallel to the substrate plane. Stopping film growth prior to formation of continuous films allowed us to image the first deposited monolayer (islands up to 500 × 500 nm) and multilayer deposits that are coherent, and molecularly flat over distances of 1−3 μm, with thicknesses of 1−5 monolayers.

We assume that Pc monolayers and multilayers whose structures are dictated by H-bonding interactions would require that most, if not all eight, of the benzamide side chains adopt a trans configuration (Figure 1c) to achieve the degree of ordering we have observed in these experiments. The presence of both isomers in powders of Pc (**1**) confirms the need to use low solution concentrations and low deposition rates, where equilibrium adsorption/desorption is achieved, to ensure that Pcs can adopt a configuration favoring the structures proposed in Figure 1. Visible absorbance spectra were obtained for thin films of Pc (**1**) on several different transparent substrates (Figure S2, Supporting Information), showing the blue shifting of the Q-band spectrum consistent with cofacial aggregation of the Pc.[56,57,68]

Thin films deposited on HOPG by chemisorption from ca. $10^{-7} - 10^{-6}$ M solutions also formed layered islands with layer-to-layer dimensions of ca. 4−5 Å or multiples thereof, consistent with the plane of the Pc parallel to the substrate plane (SI section, Figure S7). The HOPG surface is not chemically modified to promote this kind of self-assembly, however, we achieve islands of Pc (**1**) of the same dimensions and chemisorption times as on modified Au surfaces. We hypothesize that previously reported defect sites on air-cleaved HOPG surfaces,[69−72] consisting of carbonyl and carboxylic acid groups, act as nucleation sites for face-on assembly of the first-deposited Pcs, through hydrogen bonding and dipolar interactions, in addition to the $\pi-\pi$ interaction between the molecule and the HOPG surface. The surface coverage of such defects is expected to be only a few percent of a monolayer, consistent with the observed need in our studies to chemisorb ordered monolayers at very low solution concentrations of Pc (**1**), allowing ample opportunity for molecules with flat-lying orientations to dominate the adsorption product. Point contact nanoscale electrical conductivity measurements on these films also support

(62) Arbeloa, F. L.; Arbeloa, T. L.; Arbeloa, I. L.; Garcia-Moreno, I.; Costela, A.; Sastre, R.; Amat-Guerri, F. *Chem. Phys.* **1998**, *236*, 331–341.
(63) Grandke, T.; Ley, L.; Cardona, M. *Phys. Rev. B* **1978**, *18*, 3847–3871.
(64) Puigmarti-Luis, J.; Minoia, A.; del Pino, A. P.; Ujaque, G.; Rovira, C.; Lledos, A.; Lazzaroni, R.; Amabilino, D. B. *Chemistry-a European Journal* **2006**, *12*, 9161–9175.
(65) Deetz, M. J.; Fahey, J. E.; Smith, B. D. *J. Phys. Org. Chem.* **2001**, *14*, 463–467.
(66) Beijer, F. H.; Sijbesma, R. P.; Vekemans, J. A. J. M.; Meijer, E. W.; Kooijman, H.; Spek, A. L. *J. Org. Chem.* **1996**, *61*, 6371–6380.
(67) Kumaran, N.; Donley, C. L.; Mendes, S. B.; Armstrong, N. R. *J. Phys. Chem. C* **2008**, *112*, 4971–4977.
(68) Kumaran, N. Ph.D. Dissertation, University of Arizona, **2008**.
(69) Kwon, S.; Vidic, R.; Borguet, E. *Carbon* **2002**, *40*, 2351–2358.
(70) Boehm, H. P. *Carbon* **2002**, *40*, 145–149.
(71) Hwang, M. S.; Lee, H. J.; Jeong, H. S.; Seo, Y. W.; Kwon, S. J. *Surf. Coat. Technol.* **2003**, *171*, 29–33.
(72) Palermo, V.; Palma, M.; Samori, P. *Adv. Mater.* **2006**, *18*, 145–164.

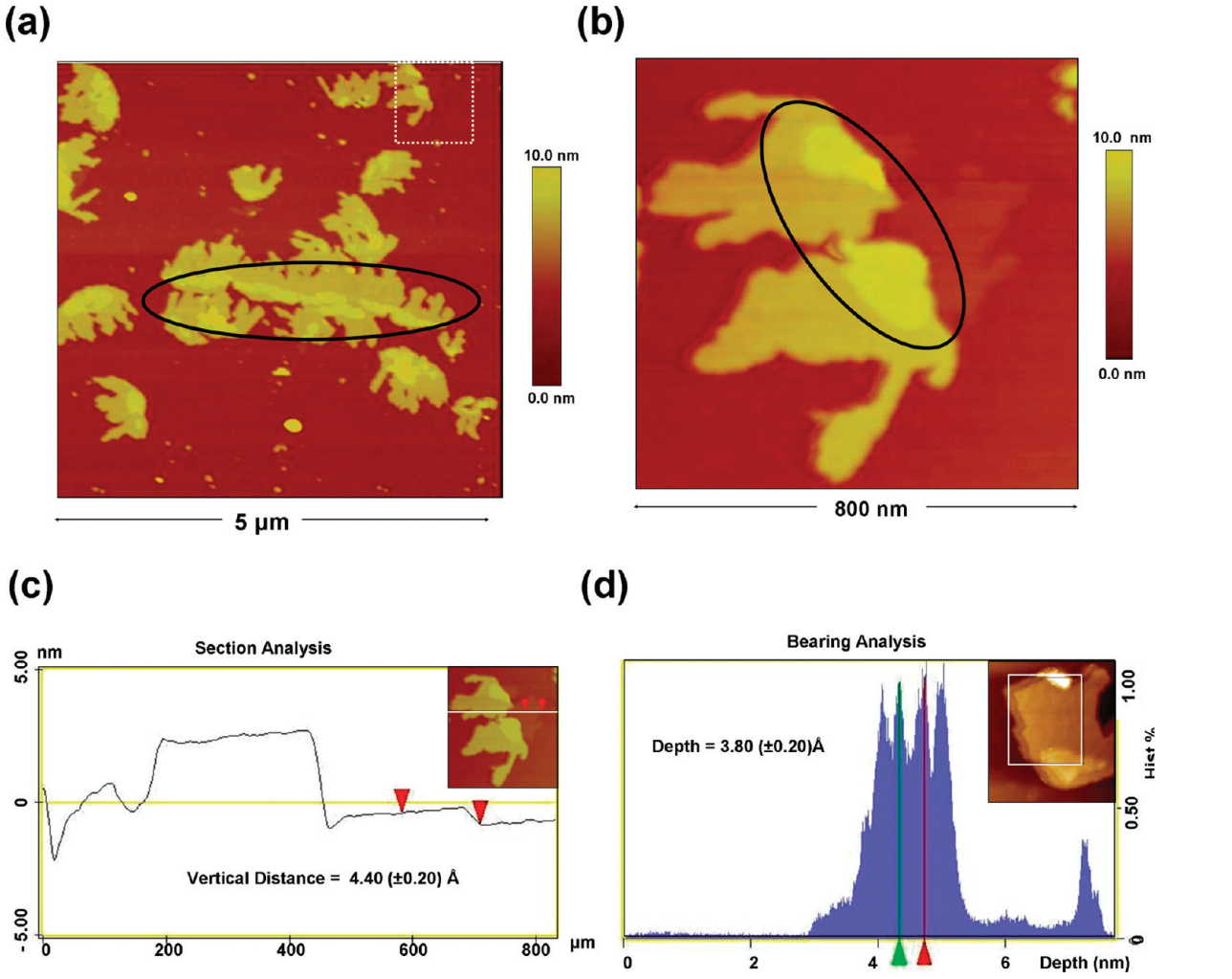

Figure 4. (a) AFM image showing layer-by-layer growth of Pc (**1**) on amide functionalized template stripped gold upon adsorption from 10^{-6} M in $CHCl_3$; some of the regions where layering is easily observed are circled. (b) High resolution image of the rectangular area in a, with thicker layers circled. (c) A typical section analysis of the film illustrates that the average monolayer thickness is ca. 4.4 Å. (d). Height histogram (bearing analysis) of a representative section the film confirms well-defined layer-by-layer growth with an average layer-to-layer distance of ~3.8 Å.

the hypothesis of layer-by-layer growth on HOPG (see below).

Layered growth of Pc (**1**) was also achieved on ITO substrates, and ITO substrates with conducting polymer overlayers such as the poly(thiophene) PEDOT:PSS.[67] Details of the growth of these thin films, characterization of their electrical properties are shown in the Supporting Information (Figures S9−11), and the use of ordered layers of Pc (**1**) as the donor layer in planar heterojunction Pc/C_{60} organic solar cells will be reported elsewhere.

Spectroscopic Characterization on Template-Stripped Gold Surfaces. Thin films of Pc (**1**) deposited on amide functionalized smooth gold were further analyzed by polarization-modulation Fourier transform infrared reflection−absorption spectroscopy (PMFT-IRRAS) to confirm the face-on alignment in the layers. The two perpendicular IR active amide modes, amide I and amide II (Figures 5a and b), have been used previously by Kim et al. to determine the orientation of peptide units in self-assembled nanotubes and nanofibers[73−75] and could be used in the characterization of these Pc assemblies as well. The amide I band, primarily due to C═O stretching, appears in the range 1610−1690 cm^{-1}, and the transition dipole moment is out of the plane of the molecule. The amide II band emerges between 1510 and 1560 cm^{-1} because of the C−N stretching and in-plane N−H bending. This transition dipole moment is in the plane of the molecule. The dichroic ratio of these absorption band intensities (amide I/amide II) was used to help assign the orientation of Pc (**1**) molecules on TSG-Au substrates, by comparison with this ratio in an isotropic sample (powders of Pc (**1**) dispersed in KBr pellets.

Figure 5c and d shows the spectra of the isotropic sample, Figure 5e and f shows the spectra of the thin films in the amide A and amide I, II regions respectively. The amide I (1654 cm^{-1}) and amide II (1537 cm^{-1}) absorption intensities of powders of **1** in the KBr pellet were nearly equal, with a dichroic ratio amide I/amide

(73) Kim, J. S.; Granstrom, M.; Friend, R. H.; Johansson, N.; Salaneck, W. R.; Daik, R.; Feast, W. J.; Cacialli, F. *J. Appl. Phys.* **1998**, *84*, 6859–6870.

(74) Paramonov, S. E.; Jun, H. W.; Hartgerink, J. D. *J. Am. Chem. Soc.* **2006**, *128*, 7291–7298.

(75) Parikh, A. N.; Allara, D. L. *J. Chem. Phys.* **1992**, *96*, 927–945.

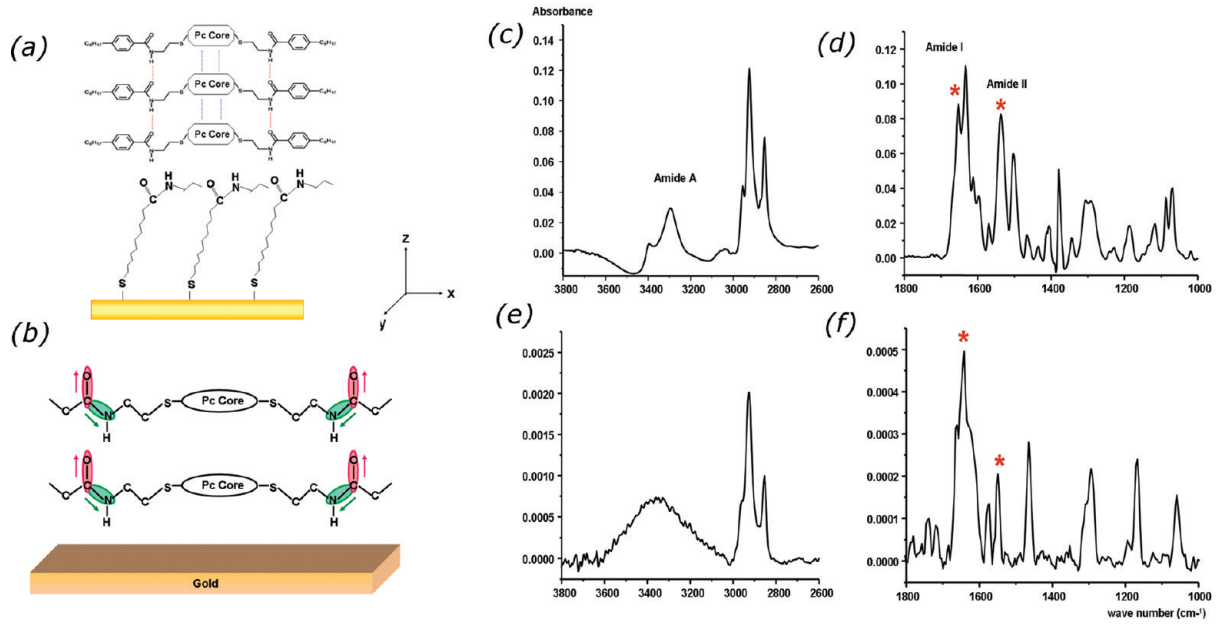

Figure 5. (a, b) Schematics of the packing arrangements proposed for Pc (**1**) on chemically modified TSG, showing the orthogonal amide I and amide II vibrational modes; (c, d) transmission IR spectrum of bulk Pc (**1**) in KBr pellet; (e, f) reflection−absorption IR spectra of Pc (**1**) thin films adsorbed on amide functionalized gold. The amide I and amide II vibrational bands are highlighted with with asterisk (*) and on modified TSG is clear that the ratio of amide I to amide II intensities favor a face-on alignment of Pc (**1**) on this substrate.

II = 1.06. In the thin film spectra the dichroic ratio amide I/amide II ≈ 2.5, suggesting a population distribution of Pcs,[67] favoring the face-on alignment observed in the AFM data of Figure 4. The broad absorption in the N−H stretching region on TSG at 3278 cm^{-1} also supports the presence of an extended hydrogen bonding network between the Pc layers.[59] A strong, broad absorption of N−H stretch in the reflection mode also signifies that the ring-to-ring H-bonding network that is exerted via the amide functional group is running perpendicular to the molecular plane.

Electrical Characterization. The electrical properties of ultrathin films of Pc (**1**) were characterized using C-AFM, which further confirmed the layer-by-layer nature of the deposition process from dilute solutions, and provided a means to measure the conductance per Pc monolayer. For these studies, Pc (**1**) was deposited on four electrically conducting substrates, HOPG (data shown in Figure 6), amide functionalized TSG, and a variety of cleaned, activated and polymer-coated ITO substrates (data for these substrates shown in Figure S9, Supporting Information). Topographic (height) images and current maps were obtained from the same analysis regions, using Pt/Ir tips.

Positive bias of the Pt/Ir tip leads to hole injection from the tip to the Pc layer, and we hypothesize that negative tip bias leads to hole injection through the Pc layer to the tip. Only slight asymmetry was observed in the $I-V$ behavior for all substrates (see also Supporting Information, Figures S10−S12). On all substrates $I-V$ plots at negative tip bias suggest thermionic emission, that is, exponential current voltage plots are obtained, especially in the high bias region.[76−78] We cannot discount the possibility of tunneling as a carrier injection mechanism, however, current densities are substantially higher for these Pc films with face-on alignment versus similar Pc films on HOPG, where the Pc rings were in edge-on alignments and tunneling through the Pc side chains appeared to dominate.[79,80] For hole injection from the Pt/Ir tip to the Pc layer at positive bias the $I-V$ curves were ohmic up to a bias of ~1 V and at higher bias best fit with a Mott−Guerney-like space-charge-limited-current (SCLC) model, that is, $I \propto V^2$.[51,76−78,81]

The height images in Figure 6 using Pt/Ir tips are not of the same quality as for the tapping mode height images shown above, but layers of Pc can still be seen, with height changes of ~4 Å or multiples thereof. $I-V$ and log $|J|-V$ responses were acquired from +1.5 V to −1.5 V using a point-contact method,[51] across the Pc layers at every ~5 nm, in 300 × 300 nm images. Only a few of these scans are shown for clarity in Figure 6. Images taken before and after the point contact $I-V$ measurements verified that no damage occurred to the Pc layer.

For biases ranging from +1.5 to 1.5 V the absolute magnitude in current changed in increments inversely proportional to the thickness of the Pc layer. This type of thickness dependent conductance has been observed before in other crystalline organic semiconductor thin films, and for self-assembled monolayers constructed

(76) Davids, P. S.; Campbell, I. H.; Smith, D. L. *J. Appl. Phys.* **1997**, *82*, 6319–6325.
(77) Chen, K. W.; Yu, Y. H.; Luo, E. Z.; Xie, Z.; Xu, J. B.; Wilson, I. H.; Bishop, W. Y.; Shen, D. S. *Chem. Phys. Lett.* **2003**, *376*, 748–752.
(78) Davids, P. S.; Kogan, S. M.; Parker, I. D.; Smith, D. L. *Appl. Phys. Lett.* **1996**, *69*, 2270–2272.
(79) Wold, D. J.; Haag, R.; Rampi, M. A.; Frisbie, C. D. *J. Phys. Chem. B* **2002**, *106*, 2813–2816.
(80) Xia, W. PhD Thesis, University of Arizona, **2005**.
(81) Shen, Y. L.; Hosseini, A. R.; Wong, M. H.; Malliaras, G. G. *ChemPhysChem* **2004**, *5*, 16–25.

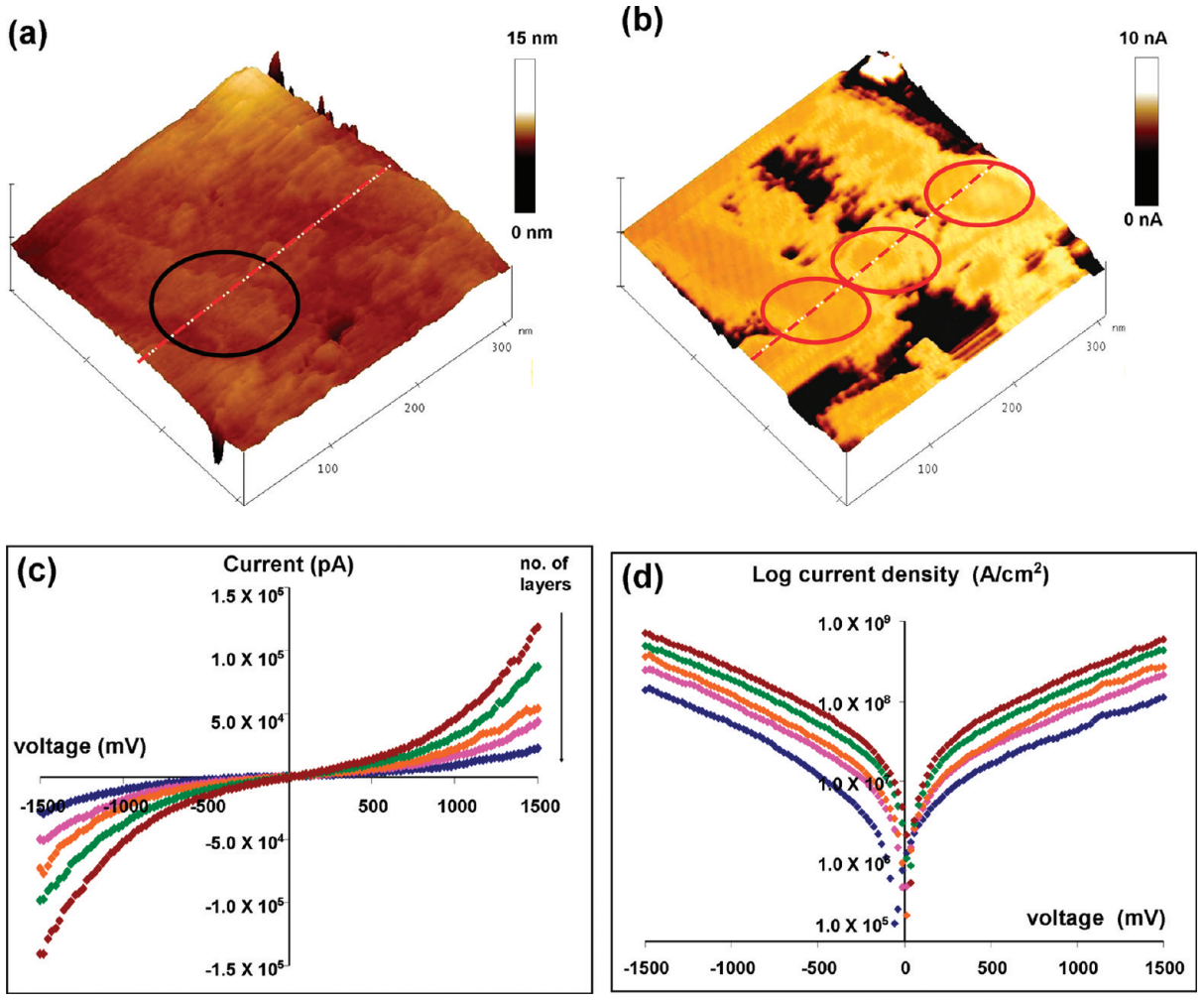

Figure 6. (a, b) C-AFM images of Pc (**1**) layers on HOPG in the height and current modes, respectively (using Pt/Ir tips). The lightest regions in the topographic images correspond to regions, where Pc films have grown in a layer-by-layer fashion (one of these regions is circled), the darkest regions in the current image correspond to the thickest Pc layers (three of these regions are circled in red), the brightest regions correspond to thinner Pc layers or bare HOPG. (c) $I-V$ plots obtained by point contact method from five different spots along the white line shown on the images The overall shape of these I−V plots remains the same, but the currents scale with Pc layer thickness, in incremental fashion. (d) log $|J|$ versus V plots (J = current density, assuming a projected tip area of ~20 nm^2) is plotted against voltage). $J-V$ plots on regions believed to be bare HOPG (not shown) produced substantially higher current densities and provided a way of discerning the boundary between the first Pc monolayer and the bare HOPG surface.

from various alkanethiols on coinage metals.[79,82,83] Such incremental changes in current density with Pc layer thickness were more difficult to obtain on the other conductive substrates, although the shapes of the current/voltage curves were comparable (Supporting Information Figures S10−S12). The current densities were actually higher for Pc films on ITO substrates, although the long-range ordering in these films was not nearly as good as seen for HOPG substrates. For the TSG substrates the added thickness of the self-assembled monolayer used to nucleate layered Pc growth added enough additional resistance so that current densities were at least a factor of 100x lower at each bias, making conductance measurements of more than 1−2 Pc layers problematic. ITO substrates with PEDOT:PSS selective layers applied before the Pc layer produced the lowest current densities and the greatest variability in $I-V$ response.

The $I-V$ behavior observed on HOPG substrates provides the opportunity to estimate contact resistance of the Pc layer.[82,83] The low bias region (−80 to −500 mV) of the five $I-V$ curves obtained from the HOPG/Pc sample was used to calculate the resistance associated with the Pc−HOPG contact. The reciprocal of the slope of the $I-V$ data (resistance) was plotted against the number of Pc layers (inset in Figure 7). The thicknesses of the Pc islands were determined from AFM section analysis, and the number of Pc layers in an island was estimated by assuming that the thinnest Pc layer observed corresponded to a single monolayer thickness 4.0 Å. We could find occasional areas of HOPG without Pc layers, and these gave much higher current densities, in an abrupt transition, as the tip moved into these bare areas, giving some confidence that we could find areas where only one monolayer of the Pc was adsorbed to HOPG.

Extrapolation of the plot in Figure 7 to zero layer thickness yielded an estimate of the Pc−HOPG contact resistance of ~8 MΩ. This value is slightly lower than the

(82) Kelley, T. W.; Frisbie, C. D. *J. Vac. Sci. Technol. B* **2000**, *18*, 632–635.
(83) Kelley, T. W.; Granstrom, E. L.; Frisbie, C. D. Adv. Mater. **1999**, *11*, 261−264.

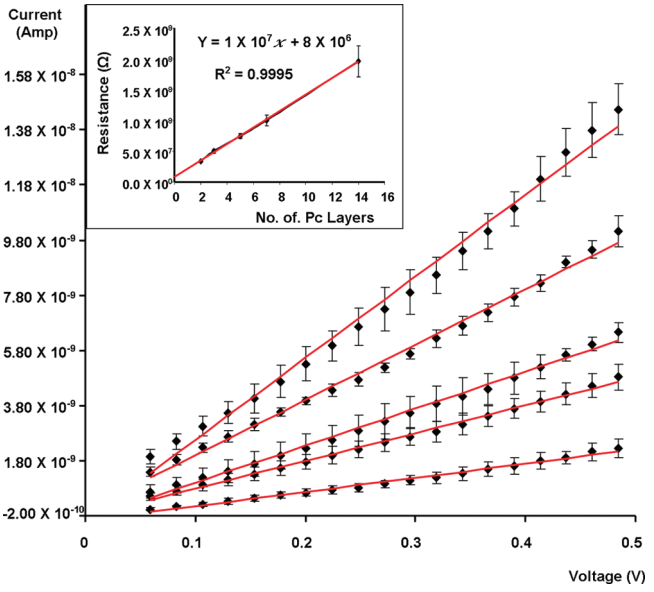

Figure 7. Expanded version of the $I-V$ plots shown in Figure 6c in the low bias region from −0.05 V to −0.5 V. Resistance of the Pc layers corresponding to these $I-V$ curves are calculated from the slope of each curves and plotted against number of layers in the inset. Extrapolation of this curve to zero Pc layers provides an estimate of the contact resistance of the Pc−HOPG heterojunction (see text).

point contact resistance estimated by Frisbie and coworkers for layered sexithiophene crystals, using a Au wire contact, and lower than our estimates for Pc assemblies with an "edge-on" thin film configuration.[80,83] From recently published data from scanning tunneling microscopy studies of discotic assemblies such as hexabenzocoronene (HBC), our I/V response, for single Pc layers appears comparable to those seen for single HBC layers on graphite.[39,84] It is interesting to note that the resistance appears to be linearly related to Pc layer thickness, rather than showing an exponential relationship. It is not clear at this time what role is played by the side chains in our assemblies, since the C-AFM tip intersects several Pc cores, and their side chains, simultaneously, including both the $\pi-\pi$ contacts in the molecular core and the more insulating contacts between side chains. This will clearly play a role in the measurement of single molecular column contact resistance, which would be enabled by these materials. Several recent studies of single molecule junctions using scanning tunneling microscopy techniques, which sample only one molecule at a time, show much higher current densities for similar bias voltages.[79,85−89] These contact resistance numbers may therefore be a high estimate of the actual contact resistance for the Pc core/HOPG interface itself.

Conclusion

Incorporation of hydrogen bonding groups in the side chains of the phthalocyanine molecules facilitates well ordered columnar aggregation and provides control over the self-assembly on surfaces. In this study, we have demonstrated a simple solution processing technique for the layer-by-layer growth of disk-like phthalocyanine molecule primarily on HOPG and surface-functionalized gold. We propose that several factors cooperatively facilitate the face-on alignment of the Pc rings to the substrate: (i) the molecular design provides for hydrogen bonding within the side chains, allowing for templating with the appropriate surface and the formation of a hydrogen bonding network of stacked Pcs; (ii) these H-bonding groups provide for interactions with even trace levels of hydrogen bond donor or acceptor sites on a variety of surfaces; (iii) deposition from extremely dilute solutions minimizes uncontrolled aggregation, but also requires low rates of deposition to sustain this ordering. AFM and FT-IR data provide evidence for formation of ordered multilayered architectures, with face-on molecular orientation.

The C-AFM images and quantized $I-V$ data seen on the Pc layers deposited on HOPG provide additional evidence for layered assembly of these Pc molecules. From our investigations of the contact behavior at metal−Pc contacts, substantially lower contact resistance at the HOPG/Pc interface implies strong molecular contacts of the Pc core with the HOPG substrate. Reasonably low contact resistances were obtained for deposition of Pc (**1**) on ITO and ITO/PEDOT:PSS substrates as well (Supporting Information), but without the long-range order seen for smoother HOPG and TSG substrates. Nevertheless we have been able to obtain Pc layers by this approach with sufficient ordering to allow their characterization as donor layers in organic solar cell, based on planar (Pc/C60) heterojunctions, which will be reported elsewhere.

Acknowledgment. This research has been supported by the National Science Foundation (CHE-0517963 (NRA) and CHE-0848624 (JEP)), the NSF Science and Technology Center-Materials and Devices for Information Technology, DMR-0120967), the Office of Naval Research, the Department of Energy Program, "Photovoltaics Beyond the Horizon" (NREL); and the Arizona Board of Regents TRIF program, Arizona Research Institute for Solar Energy (AzRISE).

Supporting Information Available: Additional AFM images and current−voltage data from C-AFM characterization of these materials. This material is available free of charge via the Internet at http://pubs.acs.org.

(84) Jackel, F.; Watson, M. D.; Mullen, K.; Rabe, J. P. *Phys. Rev. B* **2006**, *73*, 045423.
(85) Chen, F.; Tao, N. J. *Acc. Chem. Res.* **2009**, *42*, 429–438.
(86) Engelkes, V. B.; Beebe, J. M.; Frisbie, C. D. *J. Phys. Chem. B* **2005**, *109*, 16801–16810.
(87) Kelley, T. W.; Frisbie, C. D. *J. Phys. Chem. B* **2001**, *105*, 4538–4540.
(88) Song, F.; Wells, J. W.; Handrup, K.; Li, Z. S.; Bao, S. N.; Schulte, K.; Ahola-Tuomi, M.; Mayor, L. C.; Swarbrick, J. C.; Perkins, E. W.; Gammelgaard, L.; Hofmann, P. *Nat. Nanotechnol.* **2009**, *4*, 373–376.
(89) Beebe, J. M.; Kim, B.; Frisbie, C. D.; Kushmerick, J. G. *Acs Nano* **2008**, *2*, 827–832.